Cancer Nanotechnology

RESEARCH Open Access

Preferential drug delivery to tumor cells than normal cells using a tunable niosome–chitosan double package nanodelivery system: a novel in vitro model

Marzenna Wiranowska[1*], Rupin Singh[2], Rana Falahat[3], Eva Williams[3], Joseph O. Johnson[4] and Norma Alcantar[3*]

*Correspondence: mwiranow@usf.edu; norma@usf.edu
[1] Department of Pathology and Cell Biology, Morsani College of Medicine, University of South Florida, 12901 Bruce B. Downs Blvd., Tampa, FL 33612, USA
[3] Department of Chemical & Biomedical Engineering, College of Engineering, University of South Florida, 4202 E. Fowler Ave. ENB 118, Tampa, FL 33620, USA
Full list of author information is available at the end of the article

Abstract

Background: We previously described the properties of a targeted drug delivery system (DDS) in a cell-free system. Here, in this comparative cell-based study (normal and tumor cells), we provide a quantitative analysis of the extracellular diffusion and intracellular localization of this DDS. This DDS consists of fluorescence-labeled paclitaxel encapsulated in non-ionic surfactant vesicles/niosomes embedded in a thermosensitive cross-linked chitosan hydrogel with an affinity for the MUC1 mucin surface antigen overexpressed on tumor cells, and designed for a sustained and controlled, localized delivery of embedded drugs. We evaluated DDS in our novel in vitro model using MatTek' glass-bottom culture plates and compared human cancer cell lines (OV2008 epithelial origin carcinoma and U373 glioma, both overexpressing MUC1) with human normal epithelial control cell lines (IMMC3 and IOSE-121 using differential contrast and confocal microscopy.

Results: Tumor cells incubated in the presence of chitosan alone or DDS-containing chitosan–niosome–paclitaxel–BODIPY 564/570, showed a prominent granular accumulation on their surface when compared to the normal cells. Quantitation of gray value light intensity of the extracellular region of chitosan alone treated OV2008 and IOSE-121 controls done by analysis of multiple radial line segments, 4 µm each, using ImageJ software showed 2 times higher intensity around the OV2008 than around normal IOSE-121 controls ($p < 0.05$). In the DDS-treated OV2008 cells, extracellular fluorescence intensity measured at different diffusion distances outside of the cells, in three different zones showed the difference in means of fluorescence intensity in these zones ($p < 0.05$) with the highest level of fluorescence near the cell surface indicating a concentration gradient, most likely driven by the high affinity of chitosan to the MUC1 receptor. Also, as chitosan alone accumulated two times more along the edge of tumor cells compared to normal cells, we found intracellular fluorescence intensity quantified at time intervals to be also 2 times higher in OV2008 than in normal IMCC3 cells ($p < 0.05$).

Conclusion: Based on the observation of the DDS preferentially targeting tumor cells, there is a potential implication for the localized delivery of therapeutic drug doses to solid tumors or post-surgical solid tumors cavities containing residual tumor cells.

Keywords: Nanodelivery, Niosomes, Chitosan, Paclitaxel, MUC1, Tumor cells, Epithelial cells, Confocal microscopy

Background

Various systems for localized controlled drug delivery to solid tumors have been developed, but the approach itself still remains highly challenging (Bisht and Maitra 2009). Potent anti-proliferative cancer chemotherapeutics are available, but they often lack specificity and selectivity in targeting tumor cells. To improve the outcomes of chemotherapy and mitigate the toxicity of anti-cancer agents, numerous research studies have focused on the development of targeted therapies. These approaches involve nanodelivery systems in which drugs are being incorporated in variety of vehicles including nanoparticles, liposomes, micro-spheres, biodegradable polymers and niosomes (Wiranowska et al. 1998; Lee et al. 2012; Williams et al. 2012, 2013; Mahajan et al. 2016; Putri et al. 2017; Salem et al. 2018).

We previously reported a niosome-based approach for a localized drug delivery, in which niosomes, non-ionic bilayer structures with a hydrophilic core and a hydrophobic outer bilayer are embedded in a chitosan gel matrix (Williams et al. 2012). Studies of this drug-delivery system in a cell-free system using fluorescent dye (5,6-carboxyfluorescein) incorporated into the niosomes provided information regarding the release kinetics of this dye. The obtained data served as a base for this follow-up study using a novel in vitro system to evaluate the nano drug delivery system (DDS) containing fluorescent paclitaxel BODIPY 564/570 encapsulated into the niosomes and embedded in a chitosan gel matrix.

Paclitaxel is used against a wide variety of tumors like ovarian cancer, breast cancer, head and neck cancers, lung cancer and prostate cancer (Armstrong et al. 2006; Hamilton and Berek 2006). Due to its high hydrophobicity it has to be administered in combination with other formulation vehicles such as polyoxyethylated castor oil also known as Kolliphor EL, which itself is known to be associated with a number of side effects including peripheral neuropathy, nephrotoxicity, aggregation of erythrocytes, hyperlipidemia and hypersensitivity (Armstrong et al. 2006; Singla et al. 2002). Encapsulation of paclitaxel in niosomes followed by their embedment in the cross-linked chitosan can potentially eliminate the need for Kolliphor EL. Therefore, this step could reduce toxicity and add an additional level of control by tuning the drug release rates to the required dose.

Chitosan is an amino-polysaccharide obtained by alkaline deacetylation of chitin polysaccharide, a natural component of shrimp or crab shells. It is a long chain polymer with its average molecular weight ranging from 3800 to 500,000 Da (Cho et al. 2005; Chenite 2001). Chitosan is a copolymer of glucosamine and *N*-acetyl glucosamine (Chenite 2001) which is digestible by lysozyme depending on the number of *N*-acetyl groups. In addition, over time, chitosan breaks down to amino sugars (Cho et al. 2005) which are harmless to the human body, and readily absorbed.

Moreover, chitosan which is mucoadhesive was reported to have an affinity for the MUC1 adhesion molecule (CD227), a cell membrane-associated large glycoprotein

mucin, which is overexpressed in most carcinoma cells (Hollingsworth and Swanson 2004). This property of chitosan may offer an additional benefit to this delivery system by enabling targeted delivery and guiding niosomes toward MUC1 overexpressing tumor cells (Falahat et al. 2015).

A variety of properties of chitosan and derivatives have been evaluated and are described elsewhere (Arfin 2017; Vecchione et al. 2016) including as an antifungal (Andersen et al. 2017), an antibacterial (Devlieghere et al. 2004), in tissue repair such as in skin (Tchemtchoua et al. 2011), or neuroprotective (Dai et al. 2013).

Chitosan as a targeted drug delivery vehicle has been evaluated in various in vitro and in vivo tumor models, e.g., pancreatic (Zeiderman et al. 2016), glioblastoma (Wang et al. 2016), breast cancer (Nayak et al. 2016; Nguyen et al. 2016; Salem et al. 2018) and others (Chowdhuri et al. 2016).

The double packaging of paclitaxel encapsulated in niosomes embedded in the thermo-gelling chitosan network cross-linked with β-glycerophosphate (BGP), provides an additional advantage of this delivery system (Fig. 1). It not only protects niosomes against external tonicity fluctuations, but also prevents uncontrollable and premature bursting of the niosomes and release of paclitaxel. Therefore, this double packaging using chitosan as the second layer stabilizes the niosomes, thereby providing a tighter control over release time and dosage.

Here, we present the evaluation of chitosan-based DDS system using a novel in vitro model to compare its capacity of targeting tumor cells in comparison to normal control cells. This in vitro model utilized MatTek culture plates consisting of two independent chambers: a centrally located chamber compatible for cell culture growth and confocal observations and an outside chamber originally described by the manufacturer as

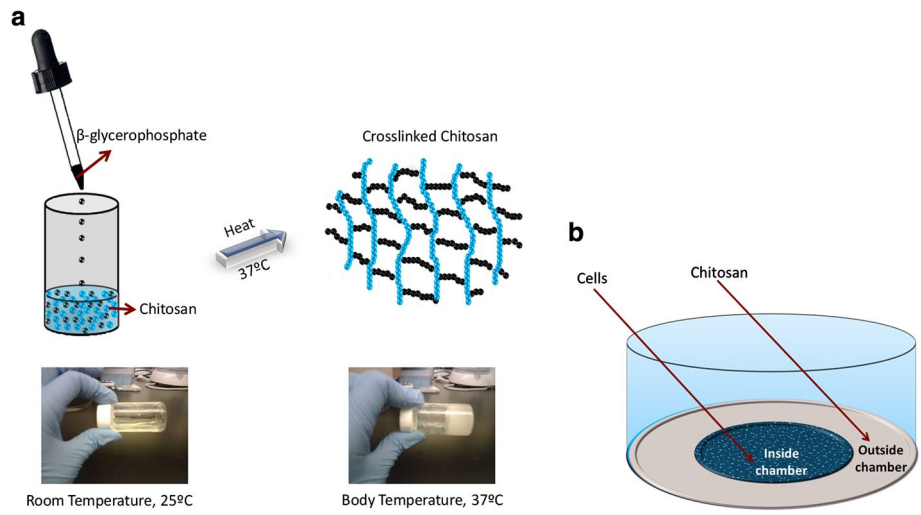

Fig. 1 **a** Preparation of cross-linked chitosan solution using the cross-linker β-glycerophosphate. The resulting solution shows thermo-responsive behavior. **b** Experimental design to test chitosan. Individual cancer cell lines (OV2008 and U373) or normal cell lines (IOSE-121 and IMCC3) were seeded in growth medium in MatTek's plates and incubated overnight. On the following day, the growth medium in the outside chamber was replaced with either fresh medium or with chitosan and all the cells were incubated for either 10 min or 1 h at 37C in 5% CO_2 and at the end of incubation plates were evaluated by confocal microscopy

a place containing an excess of the culture medium to place the DDS polymer system. These two independent chambers do not communicate with each other, but the outside chamber can serve as an additional space for the grow medium that can overflow to the center chamber during long time cell culture incubations. We used the outside chamber lined with the sterile aluminum foil for a temporary location of the DDS system (pulse treatment) which normally remains as a liquid at room temperature, but it solidifies in 37 °C in cell culture conditions. Therefore, the DDS polymer system could not be placed directly over the cells blocking their function. Instead, the DDS was placed in the outside chamber and contained within the sterile aluminum foil covering the DDS with the growth medium. That provided us with the flexibility to remove the DDS in a sterile fashion together with the foil after 15 min pulse treatment leaving some amount of DDS and allowing some of the DDS fragments to break off and diffuse in the growth medium reaching the cultured cells in the center chamber. Using this two-chamber cell culture system for the DDS delivery, we added another dimension to this in vitro system. Using confocal microscopy, we were able to observe single cells while small fragments of the DDS system diffused gradually toward the center chamber. In addition, testing the DDS-containing fluorescent paclitaxel BODIPY 564/570 in this system with cells plated in the inner chamber and the polymer injected into the outer chamber allowed for controlled amount of the DDS being delivered gradually to the center chamber without overwhelming the cells as this system lacks a natural clearance mechanisms as they are present in in vivo models. To the best of our knowledge this type of in vitro model developed by us and used for the evaluation of the chitosan/noisome/DDS system is being reported for the first time and may serve as a base for further studies.

Results

In vitro study of chitosan polymer alone

Chitosan was dissolved in 0.1 M HCl to render its free amino groups readily available for cross-linking with β-glycerophosphate. This, in turn, results in a pH increase to the physiological range of 7.0–7.4 (Williams et al. 2012). This procedural step also allows for controlled hydrogel formation when temperature increases to human body temperature of 37 °C. Therefore, in our study the chitosan-β-glycerophosphate system remained a liquid at room temperature of 25 °C, but it formed a gel when placed in the tissue culture incubator set at body temperature (Ruel-Gariépy et al. 2000; Cho et al. 2005) (Fig. 1a).

The property of chitosan described above allowed it to be dispensed as a liquid into the outer chamber of glass-bottom culture dishes (MatTek's plates) surrounding the inside chamber that contained growing adherent cells (Fig. 1b). Next, the MatTek's plates were placed in the tissue culture incubator at 37 °C for 3 min facilitating cross-linking of chitosan and resulting in chitosan forming gel in the outer chamber. The growth media added to the inside chamber of the MatTek's plates that covered the cells (OV2008 and IOSE-121) also covered the chitosan polymer in the outside chamber. Small fragments of the polymer gradually broke off and diffused toward the center of the MatTek's plate with attached growing cells while incubated at 37 °C in 5% CO_2. The observations were made of the live cells and differential interference contrast (DIC) microscopy images were captured after 10 min and 1 h of incubation. Those time points were chosen based

on the observation that longer incubation times with chitosan interfered with the possibility to observe the single cells due to chitosan accumulation.

When OV2008 were incubated in presence of chitosan for 10 min (Fig. 4c) or 1 h (Fig. 2c, d and Additional file 1), a granular layer, presumably chitosan, was seen to accumulate on the surface of the cell membrane forming a visible aura. This was not observed using growth medium alone (Fig. 2f).

However, when normal IOSE-121 cells were incubated in presence of chitosan, only small clumps of chitosan granules were seen away from the cell surface and with only a moderate amount of a granular accumulation on the cell surface after 1 h (Fig. 2a, b and Additional file 1), but not after 10 min (Fig. 4a) or using growth medium alone (Fig. 2e).

Quantitative analysis of chitosan accumulation around the tumor and normal cells following 1 h of incubation was based on the mean grey value intensity in the 4-μm zone around cells (Fig. 2b, d). Accumulation was significantly higher ($p < 0.05$) around OV2008 tumor cells (intensity mean value: 890.1) than around IOSE-121 normal cells (intensity mean value: 508.2) (Fig. 2g). This supports our observation of enhanced accumulation of chitosan around OV2008 in the extracellular space, i.e., in the immediate vicinity of cells, when compared to than IOSE-121 cells (Fig. 2a, c) and to the cells incubated in medium alone (Fig. 2e, f).

In vitro evaluation of chitosan–niosome–paclitaxel BODIPY 564/570 system

a) Paclitaxel BODIPY 564/570: before and after encapsulation

Next, we focused on the evaluation of the chitosan polymer with embedded niosomes encapsulated with paclitaxel BODIPY 564/570 compared to the paclitaxel alone. Again, we used MatTek's plates with cells seeded in the inner chamber and the chitosan–niosome–paclitaxel BODIPY 564/570 placed in the outer chamber (Fig. 3a) as described in "Methods" section. The chitosan–niosome–paclitaxel BODIPY 564/570 system was designed to slowly release niosomes while chitosan polymer disintegrated and its fragments broke off slowly diffusing toward the inner chamber that contained the cells. The

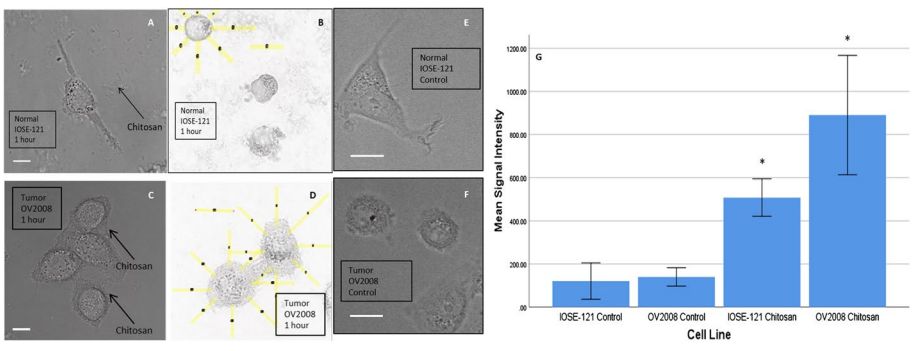

Fig. 2 Chitosan diffusion: **a**, **b** IOSE-121 normal cells incubated for 1 h in the presence of chitosan. **c**, **d** OV2008 tumor cells incubated for 1 h in the presence of chitosan. **e**, **f** IOSE-121 and OV2008 incubated in medium only. **g** Mean DIC signal intensity shows 1.75 times higher levels of intensity around OV2008 cells than around IOSE-121 cells. The background signal intensity is represented by the cell controls incubated in the medium alone. Error bars: ±1 SD. *Represents statistically significant difference (unpaired *t*-test, $p < 0.05$)

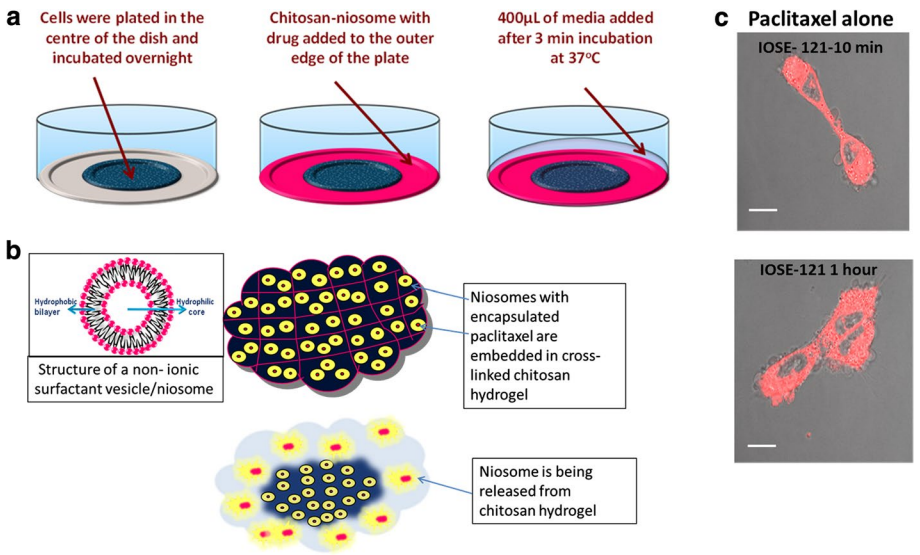

Fig. 3 **a** Experimental design to test chitosan–noisome drug delivery model using MatTek's plates. This design allowed the cells to incubate before the drug delivery system was added and allowed chitosan to polymerize at 37 °C. This novel testing model was used to evaluate our drug delivery system using different concentrations of paclitaxel and in long-term studies in both normal and tumor cells. **b** Schematic representation of the drug delivery system for localized delivery of chitosan–niosome with encapsulated paclitaxel conjugated with BODIPY 564/570. **c** Images showing IOSE-121 normal cells incubated for 10 min and 1 h in growth medium containing paclitaxel (0.4 µM) conjugated to red–orange fluorescent BODIPY 564/570

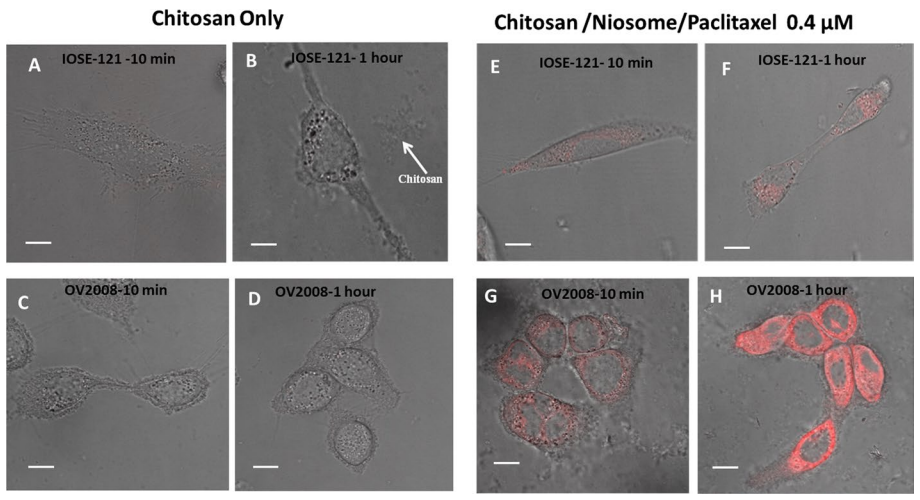

Fig. 4 **a**–**d** Images showing cells incubated in presence of chitosan: **a**, **b** IOSE-121 normal cells or **c**, **d** OV2008 tumor cells incubated for 10 min and 1 h. **e**–**h** Images showing cells incubated with chitosan/noisome/paclitaxel (0.4 µM) system: **e**, **f** IOSE-121 normal cells or **g**, **h** OV2008 tumor cells incubated for 10 min and 1 h. Scale bar = 10 µm

niosomes released from the degrading chitosan polymer (summarized in Fig. 3b) would burst following their contact with growth medium and would release the encapsulated paclitaxel BODIPY 564/570.

We first compared the effect of paclitaxel BODIPY 564/570 at 0.4 μM concentration (the highest concentration used in these experiments) added directly to the culture medium (Fig. 3c) or as a component of the chitosan–niosome polymer added for a brief observation of few minutes (< 10 min and 1 h) to MatTek plates seeded with normal IOSE-121 cells. As expected we found a high level of intracellular fluorescence from paclitaxel BODIPY 564/570 alone diluted in the growth medium (Fig. 3c) while either no or only very light cellular staining was observed from the paclitaxel encapsulated in the chitosan–niosome complex incubated for 10 min or 1 h (Fig. 4a–h). Thus, the fluorescence emitted by paclitaxel is indirect evidence of the presence of niosomes.

b) Encapsulated paclitaxel BODIPY 564/570 in chitosan–niosome system at 0.4 μM concentration

Human tumor cells lines OV2008 and U373 cells, seeded in the inner chamber of MatTek's plates, were exposed up to 1 h to the chitosan–niosome–paclitaxel BODIPY 564/570 (at 0.4 μM concentration), which was placed in the outer chamber of MatTek's plates (Fig. 5). As mentioned before, the embedded niosomes were released while fragments of chitosan broke off and diffused from the outer chamber toward the inner chamber containing the cells. Confocal microscopy images obtained at the end of incubation times showed a granular accumulation, presumably chitosan, present around the cell surface of U373 (Fig. 5a) and OV2208 (Fig. 5b) tumor cells. Both types of tumor cells emitted an intense intracellular fluorescence signal at 564/570 nm, indicating that the paclitaxel BODIPY 564/570 had been released from niosomes and taken up by the tumor cells. Therefore, this observation indirectly confirmed that the granular accumulation around the tumor cells seen on confocal microscopy were in fact chunks of the chitosan complex containing the niosomes with encapsulated fluorescence conjugated paclitaxel. This observation also confirmed that the fragments of the chitosan–niosome–paclitaxel BODIPY 564/570 complex, which diffused toward the inner chamber containing the

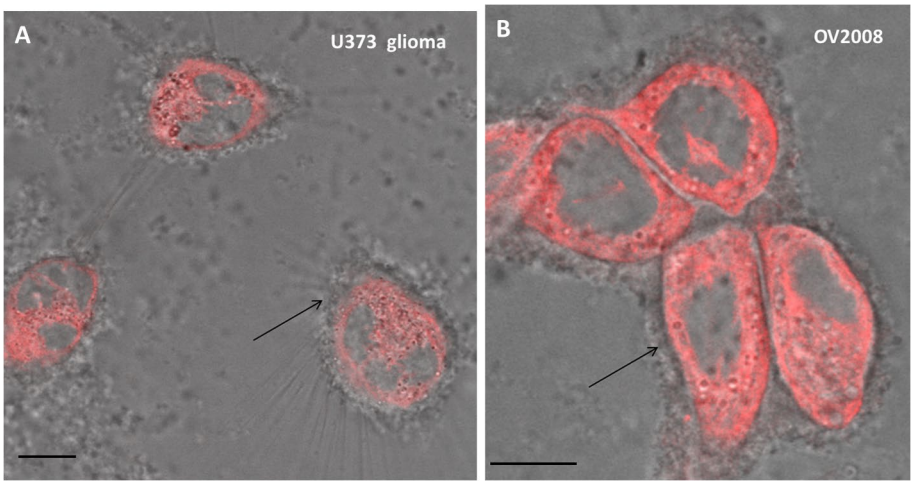

Fig. 5 Accumulation of chitosan around tumor cells following their incubation with paclitaxel–BODIPY 564/570–chitosan–niosome complex. Cells were treated for 20 min to 1 h with chitosan/paclitaxel (0.4 μM) conjugated to red–orange fluorescent BODIPY 564/570. Scale bar = 10 μm

tumor cells, released fluorescence conjugated paclitaxel near the cell surface resulting in cellular uptake and a strong intracellular fluorescent signal measured at 564/570 nm.

c) Encapsulated paclitaxel BODIPY 564/570: testing various concentrations in vitro

The aim of this study was to establish and select the optimal concentration of paclitaxel BODIPY 564/570 encapsulated into the chitosan–niosome system, which could be applied in vitro in the long-term studies (over 24 h) in subtoxic concentration. Our primary criteria for selecting the optimal concentration for long-term studies was to decide which concentration showed the lowest level of detectable cellular fluorescence after incubation for 1 h. OV2008 tumor cells seeded in MatTek's plates were incubated with preparations of the chitosan–niosome system containing three different concentrations of encapsulated paclitaxel BODIPY 564/570: 0.4, 0.04, and 0.01 μM. The confocal images of the cells showed a dose-dependent fluorescence intensity with a sufficiently high measurable level of fluorescence signal at the lowest 0.01 μM concentration (Fig. 6 and Additional file 1). Thus, the 0.01 μM concentration of paclitaxel BODIPY 564/570 was selected for the further long-term study using a 15-min pulse treatment and followed by 24 h incubation (described below in e). The confocal images obtained from this long-term study showed a detectable fluorescence signal within the cells gradually increasing with time during 24 h incubation (Additional file 1: Figure S12).

d) Wheat germ agglutinin Oregon Green-488 staining of cell membrane

To confirm the interaction of chitosan–niosome–paclitaxel BODIPY 564/570 at 0.01 μM concentration with tumor cells during long-term studies (over 24 h using 15 min pulse treatment), both OV2008 tumor cells and normal epithelial IMCC3 cells were evaluated via cell membrane staining with wheat germ agglutinin (WGA). Fluorescent lectins such as WGA Oregon Green 488 are versatile probes for detecting glycoconjugates and for localizing glycoproteins in live, cultured, adherent cells. Wheat germ agglutinin selectively binds to *N*-acetylglucosamine and *N*-acetylneuraminic acid (sialic acid) residues.

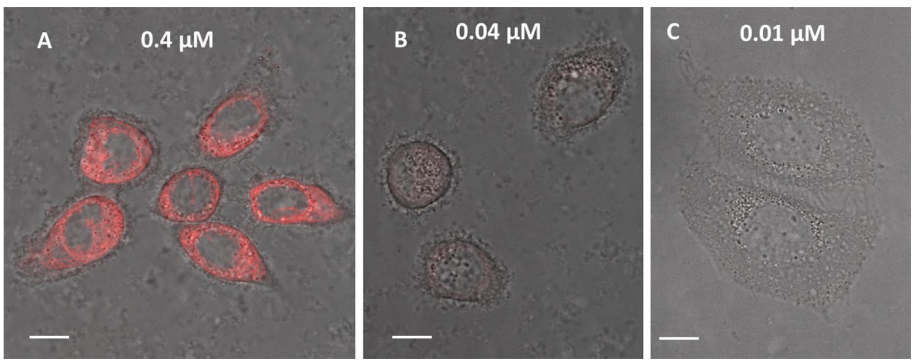

Fig. 6 Comparison of the fluorescence intensity of various concentrations of DDS complex following paclitaxel uptake. Paclitaxel–BODIPY 564/570–chitosan–niosome uptake by OV2008 cells at concentrations 0.4 μM, 0.04 μM, and 0.01 μM after 1 h of incubation (the images showing the cells following 10 min incubation with DDS containing all three concentrations of paclitaxel are found in Additional file 1). Scale bar = 10 μm

We found that both the cell membrane and chitosan complex stained with WGA-Oregon-Green-488 (Fig. 7a–d). Both cell controls for IMCC3 (Fig. 7a) and OV2008 (Fig. 7c) with only growth medium present during incubation, showed distinct staining of their cell's membrane. However, OV2008 tumor cells treated with the chitosan–niosome system showed an intensely fluorescent granular aura of chitosan around the cell body while in the normal IMCC3 cells culture the granular fluorescently stained chitosan was distant to the cell membrane and only visible away from the cell. The results of this study using chitosan–niosome–paclitaxel BODIPY 564/570 system paralleled our observation of chitosan alone showing chitosan accumulation around the tumor cells (Fig. 2).

e) Confocal microscopy and direct fluorescence evaluation: measurement and quantitation of paclitaxel fluorescent signal.

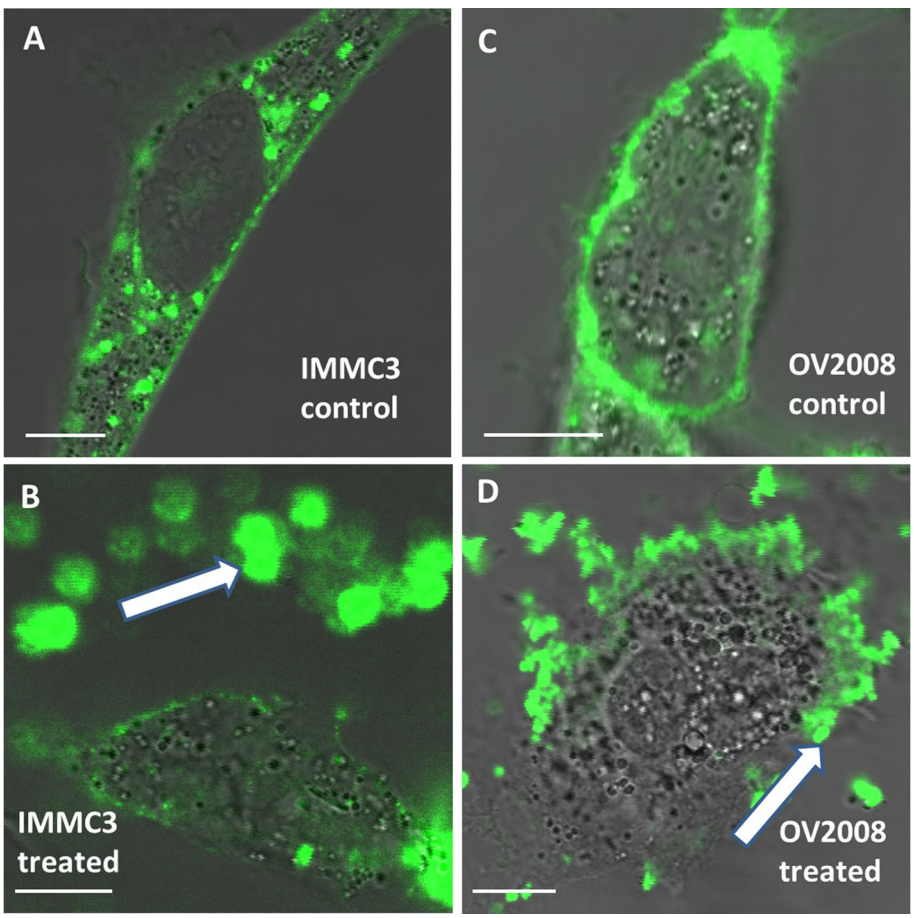

Fig. 7 Wheat germ agglutinin (WGA) Oregon Green 488 conjugate cell membrane staining. **a**, **c** Control samples without chitosan–paclitaxel showed WGA staining on the cell membranes only. **b**, **d** Treated samples with chitosan–paclitaxel at 0.01 μM following 15 min pulse treatment. WGA staining visible on cell membranes and on the chitosan polymer. Visible accumulation of chitosan polymer seen around OV2008 (**d**) while much of the chitosan was in the extracellular space around IMMC3 (**b**). Scale bar = 10 μm

The results from our experiments regarding the optimal 0.01 μM concentration of paclitaxel BODIPY 564/570 for long-term incubation studies and our observation that the chitosan complex has a higher affinity for the tumor cells than for the normal cells served as a base for designing further studies in which we compared the levels of fluoresce intensity in normal cells and tumor cells in three separate experiments. We used chitosan–niosome–encapsulated paclitaxel BODIPY 564/570 at a concentration of 0.01 μM for a 15 min pulse treatment of the OV2008 carcinoma and normal epithelial IMCC3 cells, followed by incubation for 5 min, and 24 h, in MatTek's plates. In each experiment the measurement of fluorescence included cells at various locations on the plate, i.e., the edges and in the center of the plate. The confocal microscopy images were captured at these time points and fluorescence intensity of the cells in the inner MatTek's plate was measured followed by statistical evaluation.

Intracellular evaluation

As already mentioned in "Methods" section, the total number of evaluated OV2008 tumor cells was: $n = 49–55$ (5 min and 24 h time points) and for normal ovarian IMCC3 cells $n = 15–17$, for both time points. A comparison of fluorescence intensity levels revealed a consistent ~2 times higher level in OV2008 carcinoma than normal IMCC3 epithelial cells with a statistical significance $p < 0.05$ at 5 min and 24 h incubation time points (Fig. 8). These data were statistically significant with the same relative difference between the normal and tumor cells despite the varying range of minimum and maximum intensity values of the fluorescent signal in each of the three independent experiments as reflected in SDs.

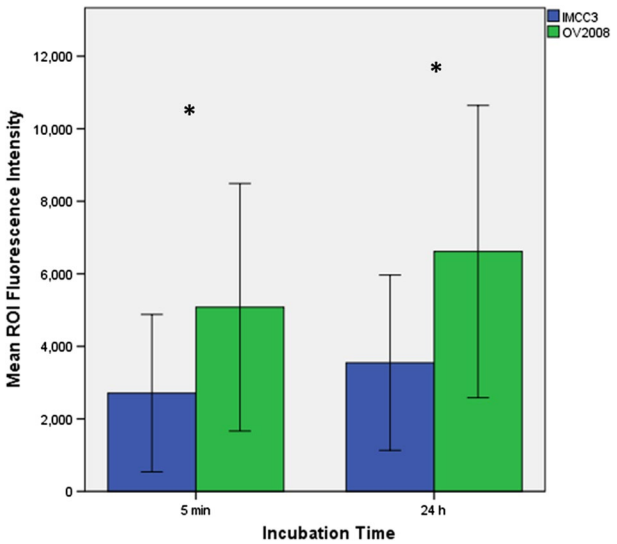

Fig. 8 Intracellular fluorescence intensity evaluation of chitosan–noisome–paclitaxel–BODIPY 564/570. Fluorescence intensity was measured at 5 min and 24 h after incubation. Approximately 2× higher fluorescence intensity was observed in OV2008 tumor cells when compared to IMMC3 normal cells. Error bars: ± 1 SD. *Represents statistically significant difference (unpaired *t*-test, $p < 0.05$)

Extracellular evaluation

The total number of evaluated OV2008 tumor cells, either found as single cells or grouped cells was: $n = 12$ (at 5 min). A comparison of the mean fluorescent intensity using ANOVA between the zones Z1–Z3 demonstrated a statistically significant ($p < 0.05$) difference at 5 min (Fig. 9). The mean fluorescence intensity values for the three zones at 5 min were 172.1 at Z1, 150.0 at Z2, and 117.5 at Z3 with Z1 being the zone closest to the cell and Z3 being the furthest away zone. This decrease in fluorescence intensity from Z1 to Z3 was consistent over all time points tested.

Discussion

In this study, we showed that the chitosan–niosome DDS, a localized drug delivery system previously evaluated by us in a cell-free system (Williams et al. 2012), was preferential in a drug delivery to the tumor cells versus normal cells. Previously, we showed in release kinetics studies in a cell-free system that chitosan–niosome, non-ionic surfactant vesicles, conjugated with 5,6-carboxyfluorescein DDS, exhibited prolonged delivery from 100 h to 55 days in a low ionic strength environment and pH conditions akin to a tumor site. The presence of chitosan is an essential part of the DDS and contributed to the effect on control of release time and dosage and stabilized the niosomes through a high ionic strength preventing uncontrolled burst of the niosomes (Williams et al. 2012).

Here, we describe a novel in vitro model for testing the DDS-containing fluorescent paclitaxel BODIPY 564/570 using MatTek's plates with cells plated in the inner chamber and the polymer injected into the outer chamber. The premise behind designing this model was to create conditions in which cells would be in the proximity of chitosan–niosome polymer, but not in direct contact. The inner glass-bottom chamber of MatTek's plates which is compatible with confocal microscopy allowed for a routine, periodic observations of live, adherent cells. The outer chamber, originally designed according to the manufacturer description to serve as a reservoir of growth medium, was used in our model as a location for liquid chitosan with its subsequent polymerization at 37 °C.

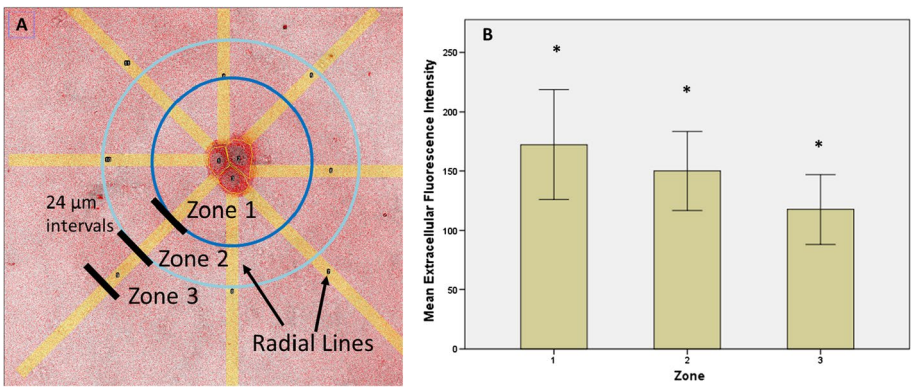

Fig. 9 Chitosan–niosome–paclitaxel-BODIPY 564/570 DDS migration zones evaluation. **a** Quantification methodology of extracellular fluorescence intensity. We used multiple radial lines split into three zones each. Zones are 24 µm in length. This methodology is meant to replicate concentric rings of equal length to help describe the DDS presence in the extracellular environment. **b** Mean fluorescence intensity at 5 min at each zone. Zone 1 showed the highest fluorescence intensity and Zone 3 showed the lowest fluorescence intensity. Error bars: ± 1 SD. *Represents statistically significant difference (ANOVA, $p < 0.05$)

As fragments of degrading DDS chitosan polymer broke off into the overlaying growth medium, we were able to observe the chitosan–niosome system diffusion toward the inner chamber containing adherent cells using confocal microscopy and DIC. The diffusing chitosan fragments containing niosomes packed with paclitaxel BODIPY 564/570 resulted in formation of a clearly visible aura around the tumor cells while it was not seen around the normal cells.

We began our studies by analyzing the diffusion of chitosan alone. Chitosan has been broadly used in the studies of pharmaceutics and tissue-engineering due to its important characteristics in drug delivery systems such as its low toxicity and bio-degradability as well as its cell and tissue compatibility (Zhang et al. 2018).

It was reported previously that chitosan is mucoadhesive and has an affinity for MUC1, a cell membrane-associated adhesion molecule (CD227), which is aberrantly overexpressed by most carcinoma cells (Hollingsworth and Swanson 2004). We found that OV2008, a tumor cell line of epithelial origin, expressed significantly higher level of MUC1 than the normal epithelial cells of the IMCC3 cell line (Falahat et al. 2015). Due to its affinity for the MUC1 receptor, a significant difference in the accumulation of chitosan around OV2008 tumor cells compared to IMCC3 normal cells was observed by differential interference contrast (DIC) microscopy and confocal microscopy. Our quantitative measurements of the gray value intensity of chitosan along the cells' edge and our observations with wheat germ agglutinin (WGA) Oregon Green 488 staining supported those findings. The mean intensity of chitosan alone in the 4 μm zone around cells was two times greater around OV2008 tumor cells than IMCC3 normal cells ($p < 0.05$).

Additionally, WGA was found to bind to both the cellular membranes and the chitosan biopolymer. The confocal microscopy images showed an observable difference in the accumulation of chitosan, as evidenced by WGA staining, around OV2008 when compared to IMCC3. WGA-stained chitosan biopolymer accumulated at the OV2008 cells' edge while in IMMC3 cultures most of it remained away from the cell membrane. Both findings support and confirm previously published data (Arfin 2017) describing properties of chitosan that suggest its usefulness as a key component of drug delivery systems targeting tumor cells.

Previously published studies using various chitosan-based chemotherapeutic drug delivery systems often evaluated tumor tissue distribution of the drug and the level of toxicity produced in the tumor cells/tissues (Lee et al. 2012; Mahajan et al. 2016; Salem et al. 2018). In contrast, our studies were designed to evaluate and compare chemotherapeutic drug delivery to tumor and normal cells at subtoxic concentrations and incubation times that would not result in cell toxicity. To the best of our knowledge this type of approach to the evaluation of drug delivery and drug uptake by the tumor and normal cells is being reported for the first time.

In our studies we used fluorescent-labeled paclitaxel BODIPY 564/570 encapsulated within niosomes and embedded into the chitosan polymer based on the fact that paclitaxel is used clinically as anti-tumor chemotherapeutic with anti-proliferative and cytotoxic activity. As the aim of our studies was to compare the effect of the chitosan–niosome system on tumor cells and normal cells measured by the level of intracellular and extracellular fluorescence, rather than cytotoxicity, we needed to establish the minimally required dose that still provides a measurable fluorescence signal. We used a short,

15 min pulse treatment with chitosan–niosome system containing the lowest concentration of paclitaxel BODIPY 564/570 (0.01 μM) and found still capable of providing a measurable fluorescent signal allowing cell observations over a period of 24 h. This 15 min pulse with the chitosan–niosome also limited the amount of chitosan–niosome–paclitaxel BODIPY 564/570 polymer remaining in the plates for the extended incubation times.

This limited presence of the locally placed chitosan–niosome system in vitro, e.g., inserts with polymer were removed from the MatTek's plates outer chamber after 15 min of incubation could be analogous to in vivo clearance of the polymer.

Our experiments showed that a prolonged presence of DDS, instead of 15 min pulse treatment would result with an overwhelming amount of polymer diffusing into the inner chamber covering cells and making it difficult to do the cell observations and measurements. Also, the selection of the 24 h for the long-term experiments using DDS-containing low concentrations of paclitaxel was determined by our preliminary studies which showed some cell loss over periods of 48 and 72 h of incubation and therefore a lower number of cells that could be evaluated in these time points.

We found here that chitosan–niosome–paclitaxel BODIPY 564/570 had a higher affinity for the tumor cells than for the normal cells based on the higher level of intracellular fluorescence intensity and presence of an extracellular fluorescence gradient around tumor cells. Just as with chitosan alone that accumulated two times more along the edge of tumor cells compared to normal cells, we found a ~2 times higher intracellular fluorescence intensity in tumor cells than normal cells ($p < 0.05$) as the tumor cells took up significantly more fluorescence conjugated paclitaxel.

To further quantify the extracellular diffusion of the chitosan–niosome–paclitaxel BODIPY 564/570 system around the tumor cells, we analyzed the extracellular fluorescence in radial segments around OV2008 tumor cells separated in three zones Z1–Z3. We showed that there is a statistically significant difference of the mean fluorescence intensity between the three zones at the initial stage of the incubation at 5 min before the chemotherapeutic intracellular uptake. We found the highest mean value of fluorescence intensity in the zone Z1, the closest to the cell surface with a decreasing fluorescence at the zones 2 and 3 (Z1 and Z2) found farther away from the cell surface. This finding is indicative of a concentration gradient most likely driven primarily by the high affinity of chitosan to the MUC1 receptor overexpressed on the tumor cells.

Conclusion

This in vitro study showed that the chitosan–niosome–paclitaxel BODIPY 564/570 DDS localized delivery system with an affinity for MUC1 receptor overexpressed on tumor cells had preferential drug delivery to tumor cells over normal cells and accumulated intracellularly and extracellularly near the cell membrane of the tumor cells, while to a lesser extent in the normal cells. The data showed a statistically significant ~2 times higher amount of extracellular chitosan as well as intracellular paclitaxel BODIPY 564/570 in tumor cells compared to normal cells when incubated at a low subtoxic concentration of 0.01 μM with a sustained release of paclitaxel observed over 24 h. Our data suggest that this DDS drug delivery system has the capacity for controlled, prolonged release of chemotherapeutics with preferential targeting of tumor cells over normal cells.

With further optimization, this model has the potential for delivering therapeutic doses to solid tumors or post-surgical solid tumors cavities thereby preferentially targeting residual tumor cells that could not be detected or removed during the debulking surgery of a solid tumor. These optimizations of the chitosan–niosome model will be performed with computational modeling and in vivo studies to better understand the pharmacodynamics and the effects of the tumor microenvironment on this system.

Methods

Materials

Paclitaxel conjugated with BODIPY® 564/570, a red–orange fluorescent dye with an excitation of 564 nm and emission of 570 nm used in this study was obtained from Invitrogen (Carlsbad, CA). Wheat germ agglutinin (WGA) Oregon Green 488 conjugate was obtained from Invitrogen, Molecular Probes (Eugene, OR). All regents used for the chitosan–niosomes were obtained from the sources described in our previous study (Williams et al. 2012).

Preparation of thermo-sensitive cross-linked chitosan solutions

Synthesis of hydrogel and process of encapsulation of niosomes was previously described by us (Williams et al. 2012). The following methodology was used. A 3 mL solution of 65% (w/v) b-glycerophosphate was added to 9 mL of 2.78% (w/v) chitosan solution (in 0.1 M HCl) drop-wise, stirring continuously over an icebath. The final solution was stirred for additional 10 min to ensure complete mixing. The final solution contained a molar ratio of 4:1 of b-glycerophosphate:chitosan. Niosomes were embedded into the chitosan network by adding niosomes into the prepared chitosan-b-glycerophosphate solution, mixing them thoroughly at 25C, and heating the resulting solution to 37C to facilitate cross-linking.

Preparation of niosomes

Niosomes preparation was done using thin-film hydration of Span-60 (sorbitan monostearate surfactant), cholesterol and dicetyl phosphate in 1:1:0.1 molar ratios in chloroform as described by Williams et al. (2012) and Williams (2012). Briefly, this solution was transferred to a round bottom flask, and the solvent was evaporated in a Buchi rotary evaporator overnight. Hydration of the film was then done with paclitaxel solutions with concentrations ranging from 2 nM to 20 mM, maintaining the evaporator's temperature at 60 °C for 1 h. Then, the solution was extruded using a polycarbonate membrane with 100 nm porous size maintaining the warm temperature and passing it through for 12 times. The hydrophobic lipophilic balance (HLB) for the niosomes prepared here falls between 4 and 8. The critical packing parameter (CPP), which is a parameter that measures the aggregation ability of amphiphiles, was 0.5–1.0 (dimensionless). The niosomes were then separated using ultracentrifugation (60,000 rpm for 40 min). The niosome was added to the preparation of the thermos-sensitive cross-linked chitosan using 0.1 M HCL chitosan solutions under ice and adding 65% v/v β-glycerophosphate cross-linker stirring for 10 min to obtain cross-link molar ratios ranging from 3:1 to 5:1.

Cells

Human epithelial carcinoma OV2008 cells recently reclassified from ovarian to cervical carcinoma cell line (Korch et al. 2012) and two primary cultures of normal human surface epithelial cells used in this study were derived from ovaries of women with no disease and no family history of breast and/or ovarian cancer that were transfected with SV-40 large T-antigen: IOSE-121 and IMCC3. These cells were kindly provided by Dr. Patricia Kruk, Department of Pathology and Cell Biology, College of Medicine, University of South Florida, Tampa. They were grown in tissue culture flasks in a 1:1 mixture of MCDB105/M199 medium (Sigma-Aldrich, MO). In addition, human glioblastoma grade III astrocytoma U373-MG (American Type Culture Collection ATCC; Manassas, VA) grown in Minimum Essential Medium was used in this study. Both growth media were supplemented with 10% heat-inactivated fetal bovine serum (Hyclone, UT), 2 mM L-glutamine, penicillin, and streptomycin. All cells were incubated at 37 °C in 5% CO_2.

In vitro study using a novel experimental model

We designed a novel in vitro system using glass-bottom microwell culture dishes (P35G-1.5 20-C.S., MatTek Corp. Ashland, MA) referred to as MatTek's plates that allow for a live cell observation using differential interference contrast (DIC) and confocal microscopy while either the chitosan or the DDS-paclitaxel BODIPY 564/570 diffusion was in progress from the outer chamber into the inner chamber with the adherent cells.

First, the cells were trypsinized and seeded in MatTek's plates according to the manufacturer's procedure at 10×10^3 cells/per MatTek's dish insert and incubated in 2 mL growth medium at 37 °C in 5% CO_2 for 24 h allowing cells to attach. The following day, the MatTek's glass-bottom culture dishes containing adherent cell cultures were removed from the incubator and either used for short-term studies (up to 1 h incubation) or for long-term studies (up to 24 h incubation).

The media at the outer edge (outside chamber—as per Figs. 1b and 3a) of the dish was pipetted out and either replaced with fresh medium in the controls or with 300 µL of liquid chitosan polymer alone or chitosan–niosome polymer system with encapsulated fluorescently tagged BODIPY 564/570 paclitaxel. The polymer was added using a syringe directly to the outer rim (in the short-term studies up to 1 h) or the sterile aluminum insert was placed first in the outer rim of the MatTek's plate and 300 µL of liquid chitosan–niosome BODIPY 564/570 paclitaxel polymer was added with the syringe (in the long-term studies). The dishes were then placed in the incubator for 3 min to facilitate cross-linking of chitosan resulting in its gelling.

For the short-term observations chitosan–niosome BODIPY 564/570 paclitaxel complex at various concentrations (0.01, 0.04 and 0.4 µM) was placed directly into the outer chamber, and followed by the addition of 400 µL of media into the inside chamber of the MatTek's plate covering the cells, as well as the polymer. The cells used for the short-term (up to 1 h) observations were OV2008 cervical carcinoma, U373 glioma, and normal ovarian epithelial cells IOSE-121 and IMCC3.

For the long-term studies, the aluminum inserts containing chitosan–niosome BODIPY 564/570 paclitaxel at 0.01 µM concentration were removed after 15 min and 400 µL of growth medium was added to the inside chamber of the MatTek's plate to

cover the cells and the polymer. With time, the small fragments of the polymer complex were gradually breaking off from the polymer located in the outside chamber and diffused toward the center of the MatTek's plate which contained seeded cells. The cell fluorescence intensity was evaluated at 5 min, and 24 h using confocal microscopy and images were captured of the cells growing both at the edge and at the center of the inner plate. Following a confocal evaluation, MatTek's dishes were returned to 37 °C at 5% CO_2 incubator.

The 15 min pulse treatment of cells with the DDS in these long-term studies (up to 24 h) limited the exposure of cells growing in this enclosed in vitro system to the DDS-containing paclitaxel–BODIPY 564/570 and therefore allowing for a gradual diffusion of chitosan polymer from an outside chamber towards the inside chamber with the cells. Direct fluorescence intensity was measured at the start of the incubation (5 min) and again at 24 h using Leica LAS AF Lite. The cells evaluated in the long-term studies were OV2008 epithelial carcinoma and normal epithelial IMCC3 cells.

Confocal microscopy and differential interference contrast (DIC) microscopy

Images of each sample (adherent cells in the MatTek's glass-bottom culture dishes) were obtained with a Leica TCS SP5 laser scanning confocal microscope (Leica Microsystems, Germany) through a 63×/1.4NA or 100×/1.4 NA. 405 Diode, argon, and helium neon (HeNe) 594 laser lines were applied to excite the samples and tunable filters were used to minimize crosstalk between fluorochromes. Gain, offset, and pinhole setting were identical for all samples within each experiment. Differential interference contrast (DIC) microscopy images were also captured using the Argon laser line. All images were taken at room temperature. The magnification for these images is 630× or 1000×. To obtain enlarged views of the cells a 3× optical zoom was applied. The scale bar shown on all images is 10 μm.

Quantitation of the extracellular chitosan alone

Measurements of the in vitro chitosan accumulation at the immediate vicinity of cells compared to the media controls were performed using the differential interference contrast (DIC) microscopy. Images were quantified with the ImageJ software (National Institutes of Health, Maryland, USA). Multiple radial directions from the cell center were taken into consideration, and grey value light intensity in the space around the cells (normalized by the background values) was measured in the line segments of 4 μm each. The results were exported to Microsoft Excel for statistical analysis.

Measurement and quantitation of extracellular and intracellular paclitaxel fluorescent light intensity

Extracellular signal

Analysis of the extracellular diffusion of paclitaxel BODIPY 564/570 around OV2008 cells was performed by quantifying the fluorescence intensity with ImageJ software (National Institutes of Health, Maryland, USA) using the confocal images. The extracellular space immediately around the cells was divided into three zones of intensity, 24 μm width each, and labeled Z1–Z3 with Z1 being the region closest to the cell. The fluorescent intensity signal was evaluated using multiple radial line segments of 30 pixels in

thickness to constitute a circular pattern around each cell. The results were exported to Microsoft Excel and IBM SPSS Statistics 24 for statistical analysis.

Intracellular signal

Analysis of each cell's fluorescence intensity resulting from the uptake of paclitaxel BODIPY 564/570 was performed and quantified with Leica LAS AF Lite software (Leica Microsystems, Germany) using the confocal images. The control plates with medium alone were used to establish "Gain" for the paclitaxel's BODIPY 564/570 fluorescence to exclude the auto fluorescence. Individual cells were segmented using the "Region of Interest" (ROI) selection tool and mean intensity of the paclitaxel signal was measured in pixels within the ROI. Results were exported to Microsoft Excel for statistical analysis.

Wheat germ agglutinin staining of the cell membrane

Wheat germ agglutinin (WGA) Oregon Green 488 conjugate from Molecular Probes with excitation at 496 nm and emission at 524 nm was used for the staining of cell membrane in live cells. Two MatTek's plates for each cell line OV2008 and IMCC3 were seeded for the long-term experiments as described above. The cells in one plate were non-treated and used as a control and the cells in the second plate were treated with chitosan–niosome–paclitaxel BODIPY 564/570 at 0.01 μM concentration with a 15 min pulse treatment in the long-term studies as described above. Following over 24 h incubation at 37 °C in 5% CO_2, the 300 μL volume of growth medium was removed from above the cells in the inner chamber of the MatTek's plate and replaced with 300 μL of WGA Oregon Green 488 conjugate solutions made in Hanks Balanced Salt Solution (HBSS) at 5 μg/mL as recommended by the manufacturer or HBSS alone for the control plates. Next, cells were incubated for 10 min at 37 °C in 5% CO_2, the labeling solution was removed, and cells were washed twice in HBSS. The cells were then observed by confocal microscopy and images were captured.

Statistical analysis

Microsoft Excel Analysis Tool Pack (Redmond, WA) and IBM SPSS Statistics (IBM Corporation, New York, USA) was used to evaluate the fluorescence intensity data.

For chitosan alone diffusion evaluation: Descriptive statistics with mean and standard deviation (SD) were obtained for intensity values for each cell at the 1 h time point of the experiment. The total number of evaluated cells in the experiment was as follows: for OV2008 $n=14$ and IOSE-121 $n=5$ (incubation with chitosan). Also OV2008 $n=7$ and IOSE-121 $n=7$ were evaluated (medium control). Determination of F value for two sample variances was followed by the appropriate (assuming unequal or equal variances) two tail Student's t test. Differences between the groups were considered statistically significant at $p<0.05$.

For intracellular fluorescence intensity evaluation: Descriptive statistics with mean and standard deviation (SD) were obtained for fluorescence intensity measured for each cell at time points 5 min and 24 h in three separate experiments. The total number of evaluated cells in all experiments was as follows: for OV2008 $n=55$ (5 min time point); $n=49$ (24 h time point), and IMCC3 $n=17$ (5 min time point), $n=16$ (24 h time point), Determination of F value for two sample variances was followed by the appropriate

(assuming unequal or equal variances) two tail Student's *t*-test. Differences between the groups were considered statistically significant at $p < 0.05$.

For the extracellular paclitaxel fluorescent signal evaluation: Descriptive statistics with mean and standard deviation (SD) were obtained for fluorescence intensity measured at time point 5 min, in two experiments. The total number of evaluated extracellular spaces defined by an area adjacent to one cell or a group of OV2008 cells was: $n = 12$. Determination of normality (normally distributed or not normally distributed sample) of each zone at each time point was completed using the Shapiro–Wilk test and followed by the appropriate analysis of multiple means (ANOVA or Kruskal–Wallis test). Differences between the zones were considered statistically significant at $p < 0.05$.

Supplementary information

Supplementary information accompanies this paper at https://doi.org/10.1186/s12645-020-00059-3.

Additional file 1. Supplemental images for IOSE-121 normal cells or OV2008 tumor cells incubated in medium alone or in presence of chitosan for 1 h. Also images of IOSE-121 normal cells or OV2008 tumor cells incubated in presence of chitosan and gray value intensity evaluated around the cells. In addition, images of OV2008 incubated with DDS at 10 min and 1 h at three different concentrations of paclitaxel and four images showing tumor cells OV2008 and normal cells incubated with the DDS using 15 min pulse treatment and evaluated at 15 min and 24 h.

Abbreviations

DDS: Drug delivery system; BGP: β-Glycerophosphate; MUC1: Mucin 1; MatTek's plates: Glass-bottom microwell culture dishes (P35G-1.5 20-C.S., MatTek Corp. Ashland, MA); DIC: Differential interface contrast microscopy; WGA: Wheat germ agglutinin; ANOVA: Analysis of variances; SD: Standard deviation; ROI: Region of interest; HBSS: Hank's balanced salt solution.

Acknowledgements

The cells OV2008, IOSE-121 and IMCC3 were kindly provided by Dr. Patricia Kruk, Department of Pathology and Cell Biology, College of Medicine, University of South, Florida. Williams, E, Ph.D. Pre-doctoral Ruth L. Kirschstein National Research Service Award from the National Cancer Institute/National Institutes of Health (NCI/NIH—F31CA145736). Singh R, MD was supported by the Scholarly Concentrations Program at USF Health, Morsani College of Medicine, Tampa, FL. Patent Application (Invention Disclosure #14A034) "Enhanced Drug Delivery System via Chitosan Hydrogel and Chlorotoxin" submitted to USF Technology Transfer Office Patent & Licensing, US Patent No 9522114 issued on December 20, 2016.

Authors' contributions

MW directed the cell based study and designed the glass-bottom culture dish (MatTek's plate) based in vitro model for the DDS system evaluation and wrote the manuscript. NA directed the study involving DDS system and developed the DDS delivery system. NA is the principal inventor on the patent issued to USF in 2016, for the DDS system. RF and EW were a graduate students of NA at the USF College of Engineering at the time of this study. They contributed to the development of the DDS system and in vitro evaluations. RS was a medical student at the time of this study and was supported by the USF Scholarly Concentration Program. He was involved in the evaluations of the extracellular levels of chitosan and DDS using ImageJ program and the statistical evaluations and was a contributor in writing the manuscript. JJ is the director of the Analytic Microscopy Core, H. Lee Moffitt Cancer Center and provided the evaluations and the images of cells in this study using both differential interference contrast microscopy and confocal microscopy. All authors read and approved the final manuscript.

Funding

Experimental studies were funded by the USF College of Engineering Interdisciplinary Scholarship Program, Tampa, FL. Signature Interdisciplinary Grant Program in Neuroscience USF, Tampa, FL. "Evaluating the Effectiveness and Biocompatibility of a Novel Drug Delivery System to Treat Brain Tumors".

Availability of data and materials

The datasets generated and/or analyses during the current study are available from the corresponding author on reasonable request.

Ethics approval and consent to participate

Not applicable (No human or animal studies).

Consent for publication

Not applicable (No data from any individual person).

Competing interests

NA (main inventor), RF and MW are co-inventors of US Patent No 9522114, "Enhanced Drug Delivery System via Chitosan Hydrogel and Chlorotoxin", issued on December 20, 2016 to USF.

Author details
[1] Department of Pathology and Cell Biology, Morsani College of Medicine, University of South Florida, 12901 Bruce B. Downs Blvd., Tampa, FL 33612, USA. [2] Scholarly Concentration: Biomedical Research, Morsani College of Medicine, University of South Florida, 12901 Bruce B. Downs Blvd., Tampa, FL 33612, USA. [3] Department of Chemical & Biomedical Engineering, College of Engineering, University of South Florida, 4202 E. Fowler Ave. ENB 118, Tampa, FL 33620, USA. [4] Analytic Microscopy Core, H. Lee Moffitt Cancer Center and Research Institute, 12902 Magnolia Dr., Tampa, FL 33612, USA.

Received: 26 June 2019 Accepted: 4 March 2020
Published online: 30 March 2020

References

Andersen T, Mishchenko E, Flaten G, et al. Chitosan-based nanomedicine to fight genital candida infections: chitosomes. Mar Drugs. 2017;15:64. https://doi.org/10.3390/md15030064.
Arfin T. Chitosan and its derivatives: overview of commercial applications in diverse fields. Chitosan: derivatives, composites and applications. Hoboken: Wiley; 2017. p. 115–49.
Armstrong DK, Bundy B, Wenzel L, et al. Intraperitoneal cisplatin and paclitaxel in ovarian cancer. N Engl J Med. 2006;354:34–43. https://doi.org/10.1056/nejmoa052985.
Bisht S, Maitra A. Dextran-doxorubicin/chitosan nanoparticles for solid tumor therapy. Wiley Interdiscip Rev Nanomed Nanobiotechnol. 2009;1:415–25. https://doi.org/10.1002/wnan.43.
Chenite A. Rheological characterisation of thermogelling chitosan/glycerol-phosphate solutions. Carbohyd Polym. 2001;46:39–47. https://doi.org/10.1016/s0144-8617(00)00281-2.
Cho J, Heuzey M-C, Bégin A, Carreau PJ. Physical gelation of chitosan in the presence of β-glycerophosphate: the effect of temperature. Biomacromolecules. 2005;6:3267–75. https://doi.org/10.1021/bm050313s.
Chowdhuri AR, Singh T, Ghosh SK, Sahu SK. Carbon dots embedded magnetic nanoparticles @Chitosan @metal organic framework as a nanoprobe for pH sensitive targeted anticancer drug delivery. ACS Appl Mater Interfaces. 2016;8:16573–83. https://doi.org/10.1021/acsami.6b03988.
Dai X, Chang P, Zhu Q, et al. Chitosan oligosaccharides protect rat primary hippocampal neurons from oligomeric β-amyloid 1-42-induced neurotoxicity. Neurosci Lett. 2013;554:64–9. https://doi.org/10.1016/j.neulet.2013.08.046.
Devlieghere F, Vermeulen A, Debevere J. Chitosan: antimicrobial activity, interactions with food components and applicability as a coating on fruit and vegetables. Food Microbiol. 2004;21:703–14. https://doi.org/10.1016/j.fm.2004.02.008.
Falahat R, Wiranowska M, Gallant ND, Toomey R, Hill R, Alcantar N. A cell ELISA for the quatification of MUC1 mucin (CD227) expressed by cancer cells of epithelial and neuroectodermal origin. Cell Immunol. 2015;298(1–2):96–103.
Hamilton CA, Berek JS. Intraperitoneal chemotherapy for ovarian cancer. Curr Opin Oncol. 2006;18:507–15. https://doi.org/10.1097/01.cco.0000239892.21161.18.
Hollingsworth MA, Swanson BJ. Mucins in cancer: protection and control of the cell surface. Nat Rev Cancer. 2004;4:45–60. https://doi.org/10.1038/nrc1251.
Korch C, Spillman MA, Jackson TA, et al. DNA profiling analysis of endometrial and ovarian cell lines reveals misidentification, redundancy and contamination. Gynecol Oncol. 2012;127:241–8. https://doi.org/10.1016/j.ygyno.2012.06.017.
Lee J-H, Oh H, Baxa U, et al. Biopolymer-connected liposome networks as injectable biomaterials capable of sustained local drug delivery. Biomacromolecules. 2012;13:3388–94. https://doi.org/10.1021/bm301143d.
Mahajan M, Utreja P, Jain SK. Paclitaxel loaded nanoliposomes in thermosensitive hydrogel: a dual approach for sustained and localized delivery. Anticancer Agents Med Chem. 2016;16:365–76. https://doi.org/10.2174/1871520615666150807103910.
Nayak D, Minz AP, Ashe S, et al. Synergistic combination of antioxidants, silver nanoparticles and chitosan in a nanoparticle based formulation: characterization and cytotoxic effect on MCF-7 breast cancer cell lines. J Colloid Interface Sci. 2016;470:142–52. https://doi.org/10.1016/j.jcis.2016.02.043.
Nguyen KT, Le DV, Do DH, Le QH. Development of chitosan graft pluronic®F127 copolymer nanoparticles containing DNA aptamer for paclitaxel delivery to treat breast cancer cells. Adv Nat Sci Nanosci Nanotechnol. 2016;7:025018. https://doi.org/10.1088/2043-6262/7/2/025018.
Putri AD, Murti BT, Sabela M, et al. Nanopolymer chitosan in cancer and alzheimer biomedical application. Chitosan. 2017. https://doi.org/10.1002/9781119364849.ch12.
Ruel-Gariépy E, Chenite A, Chaput C, et al. Characterization of thermosensitive chitosan gels for the sustained delivery of drugs. Int J Pharm. 2000;203:89–98. https://doi.org/10.1016/s0378-5173(00)00428-2.
Salem HF, Kharshoum RM, El-Ela FIA, et al. Evaluation and optimization of pH-responsive niosomes as a carrier for efficient treatment of breast cancer. Drug Deliv Transl Res. 2018;8:633–44. https://doi.org/10.1007/s13346-018-0499-3.
Singla AK, Garg A, Aggarwal D. Paclitaxel and its formulations. Int J Pharm. 2002;235:179–92. https://doi.org/10.1016/s0378-5173(01)00986-3.
Tchemtchoua VT, Atanasova G, Aqil A, et al. Development of a chitosan nanofibrillar scaffold for skin repair and regeneration. Biomacromolecules. 2011;12:3194–204. https://doi.org/10.1021/bm200680q.
Vecchione R, Quagliariello V, Calabria D, et al. Curcumin bioavailability from oil in water nano-emulsions: in vitro and in vivo study on the dimensional, compositional and interactional dependence. J Control Release. 2016;233:88–100. https://doi.org/10.1016/j.jconrel.2016.05.004.
Wang G, Wang J-J, Tang X-J, et al. In vitro and in vivo evaluation of functionalized chitosan–pluronic micelles loaded with myricetin on glioblastoma cancer. Nanomed Nanotechnol Biol Med. 2016;12:1263–78. https://doi.org/10.1016/j.nano.2016.02.004.
Williams EC (and N. Alcantar-Thesis supervisor). Smart packaging: a novel technique for localized drug delivery for ovarian cancer. Dissertation, Tampa, Florida, University of South Florida. 2012. http://scholarcommons.usf.edu/etd/4257).

Williams EC, Toomey R, Alcantar N. Controlled release niosome embedded chitosan system: effect of crosslink mesh dimensions on drug release. J Biomed Mater Res Part A. 2012;100A:3296–303. https://doi.org/10.1002/jbm.a.34275.
Williams EC, Alcantar N, Wiranowska M. Nano-particle based delivery of therapeutics to glioma. In: Wiranowska M, Vrionis FD, editors. Gliomas: symptoms, diagnosis and treatment options. New York: Nova Science Publishers Inc; 2013.
Wiranowska M, Ransohoff J, Weingart JD, et al. Interferon-containing controlled-release polymers for localized cerebral immunotherapy. J Interferon Cytokine Res. 1998;18:377–85. https://doi.org/10.1089/jir.1998.18.377.
Zeiderman MR, Morgan DE, Christein JD, et al. Acidic pH-targeted chitosan-capped mesoporous silica coated gold nanorods facilitate detection of pancreatic tumors via multispectral optoacoustic tomography. ACS Biomater Sci Eng. 2016;2:1108–20. https://doi.org/10.1021/acsbiomaterials.6b00111.
Zhang L, Chen F, Zheng J, et al. Chitosan-based liposomal thermogels for the controlled delivery of pingyangmycin: design, optimization and in vitro and in vivo studies. Drug Deliv. 2018;25:690–702. https://doi.org/10.1080/10717544.2018.1444684.

Publisher's Note